



Aortic valve calcification and myocardial fibrosis determine outcome following transcatheter aortic valve replacement

Ruben Evertz^{1,2} , Sebastian Hub^{1,2}, Bo Eric Beuthner^{1,2}, Sören J. Backhaus^{1,2}, Torben Lange^{1,2}, Alexander Schulz^{1,2}, Karl Toischer^{1,2}, Tim Seidler^{1,2}, Stephan von Haehling^{1,2}, Miriam Puls^{1,2}, Johannes T. Kowallick³, Elisabeth M. Zeisberg^{1,2}, Gerd Hasenfuß^{1,2} and Andreas Schuster^{1,2*} 

¹Department of Cardiology and Pneumology, University Medical Center Göttingen (UMG), Georg August University of Göttingen, Göttingen, Germany; ²German Center for Cardiovascular Research (DZHK), Partner Site Göttingen, Germany; and ³Department of Diagnostic and Interventional Radiology, University Medical Center Göttingen (UMG), Georg August University of Göttingen, Göttingen, Germany

Abstract

Aims There is evidence to suggest that the subtype of aortic stenosis (AS), the degree of myocardial fibrosis (MF), and level of aortic valve calcification (AVC) are associated with adverse cardiac outcome in AS. Because little is known about their respective contribution, we sought to investigate their relative importance and interplay as well as their association with adverse cardiac events following transcatheter aortic valve replacement (TAVR).

Methods and results One hundred consecutive patients with severe AS and indication for TAVR were prospectively enrolled between January 2017 and October 2018. Patients underwent transthoracic echocardiography, multidetector computed tomography, and left ventricular endomyocardial biopsies at the time of TAVR. The final study cohort consisted of 92 patients with a completed study protocol, 39 (42.4%) of whom showed a normal ejection fraction (EF) high-gradient (NEFHG) AS, 13 (14.1%) a low EF high-gradient (LEFHG) AS, 25 (27.2%) a low EF low-gradient (LEFLG) AS, and 15 (16.3%) a paradoxical low-flow, low-gradient (PLFLG) AS. The high-gradient phenotypes (NEFHG and LEFHG) showed the largest amount of AVC (807 ± 421 and 813 ± 281 mm³, respectively) as compared with the low-gradient phenotypes (LEFLG and PLFLG; 503 ± 326 and 555 ± 594 mm³, respectively, $P < 0.05$). Conversely, MF was most prevalent in low-output phenotypes (LEFLG > LEFHG > PLFLG > NEFHG, $P < 0.05$). This was paralleled by a greater cardiovascular (CV) mortality within 600 days after TAVR (LEFLG 28% > PLFLG 26.7% > LEFHG 15.4% > NEFHG 2.5%; $P = 0.023$). In patients with a high MF burden, a higher AVC was associated with a lower mortality following TAVR ($P = 0.045$, hazard ratio 0.261, 95% confidence interval 0.07–0.97).

Conclusions MF is associated with adverse CV outcome following TAVR, which is most prevalent in low EF situations. In the presence of large MF burden, patients with large AVC have better outcome following TAVR. Conversely, worse outcome in large MF and relatively little AVC may be explained by a relative prominence of an underlying cardiomyopathy. The better survival rates in large AVC patients following TAVR indicate TAVR induced relief of severe AS-associated pressure overload with subsequently improved outcome.

Keywords Aortic valve calcification; Myocardial fibrosis; Transcatheter aortic valve replacement

Received: 27 July 2022; Revised: 3 December 2022; Accepted: 4 January 2023

*Correspondence to: Andreas Schuster, Department of Cardiology and Pneumology, University Medical Center Göttingen (UMG), Georg August University of Göttingen, Robert-Koch-Str. 40, 37099 Göttingen, Germany. Tel: +49 551 39 20870; Fax: +49 551 39 22026. Email: andreas_schuster@gmx.net

Introduction

Aortic stenosis (AS) is the most common valvular heart disease in the elderly population in Europe and North America.^{1,2} Four subtypes of AS are defined by differences

in ejection fraction (EF) as well as the resulting transvalvular gradient: normal EF high-gradient (NEFHG) AS, low EF high-gradient (LEFHG) AS, low EF low-gradient (LEFLG) AS, and paradoxical low-flow, low-gradient (PLFLG) AS.

In absence of a high-gradient situation, defined as $V_{\max} \geq 4$ m/s or $P_{\text{mean}} \geq 40$ mmHg, the diagnostic workup is challenging. Besides a dobutamine stress echocardiography, multidetector computed tomography (MDCT) has gained increasing importance to discriminate between severe and non-severe AS using the estimated aortic valve calcification (AVC).^{1,3}

In addition to diagnostic capabilities, MDCT has also proven prognostic implications. Registry data demonstrate that high amounts of AVC are associated with increased mortality in patients with severe AS who did not consistently receive aortic valve replacement.^{4–7} However, there are only limited data on the prognostic value of AVC following aortic valve replacement. Some evidence suggests that LEFLG AS with higher amounts of AVC has better survival rates compared with LEFLG AS with lower amounts of AVC following transcatheter aortic valve replacement (TAVR). This is most likely attributed to disease-specific treatment in the group with large calcium burden.⁸ Conversely, in patients with severe AS, an unfavourable myocardial tissue composition with extensive myocardial fibrosis (MF) is associated with worse outcomes.^{9,10}

At present, it is still unclear how the degree and distribution of AVC relate to changes in myocardial tissue composition as well as they may determine a certain cardiac phenotype, which may or may not recover after pressure relief following TAVR. Although both AVC and MF seem to be essential keys in long-term outcome in AS, there are currently no studies looking at both parameters trying to elucidate their relative importance in TAVR patients. Therefore, we sought to investigate AVC distribution of the aortic valve and MF content of the left ventricular (LV) to better understand the pathophysiology of the different AS subtypes as well as to better delineate the relative merits of these parameters for clinical use.

Methods

One hundred consecutive patients, who underwent transfemoral TAVR, were prospectively enrolled between January 2017 and October 2018. The severity of the AS was measured according to current guidelines, and the indication for TAVR was confirmed by the local heart team.¹

The study protocol has been previously described.¹¹ At baseline, transthoracic and transoesophageal echocardiography (TTE and TOE) and MDCT were performed. Exercise capacity was measured by a 6 min walk test (6MWT). For calculating the pressure relief following TAVR, all patients underwent a second TTE at discharge. Cardiovascular (CV) mortality was defined according to the Valve Academic Research Consortium 3 consensus document (VARC-3).¹² Mean follow-up period was 322 ± 169 days following TAVR. After

the database was closed, eight patients were excluded from further evaluation. Four of them were retrospectively classified as moderate-to-severe AS, and four patients did not undergo MDCT due to an emergency TAVR (Figure 1). Therefore, the final study cohort consisted of 92 patients with a completed study protocol.

The local ethics committee approved the study, and written informed consent was obtained from all patients. The study was conducted according to the principles of the Declaration of Helsinki.

Echocardiography

All patients received a standardized TTE and TOE using either a Philips ie33 or a Philips Epiq7 system. Post-processing and severity measurements were performed by a physician specialist in echocardiography using Philips Q-Station 3.8.5.

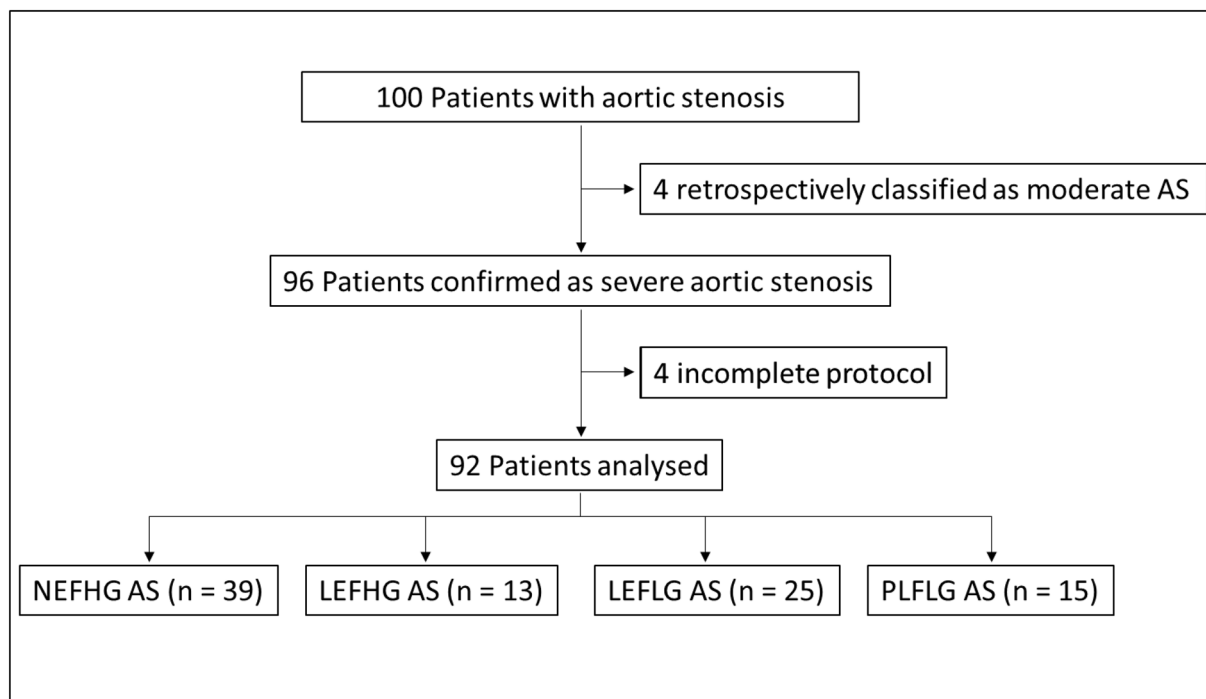
AS was categorized according to current guidelines in four subtypes, defined as follows¹:

- NEFHG AS: LVEF $\geq 50\%$, $V_{\max} \geq 4$ m/s or $P_{\text{mean}} \geq 40$ mmHg, and aortic valve area (AVA) ≤ 1 cm².
- LEFHG AS: LVEF $< 50\%$, $V_{\max} \geq 4$ m/s or $P_{\text{mean}} \geq 40$ mmHg, and AVA ≤ 1 cm².
- LEFLG AS: LVEF $< 50\%$, $V_{\max} < 4$ m/s or $P_{\text{mean}} < 40$ mmHg, and AVA ≤ 1 cm² and stroke volume index ≤ 35 mL/m².
- PLFLG AS: LVEF $\geq 50\%$, $V_{\max} < 4$ m/s or $P_{\text{mean}} < 40$ mmHg, AVA ≤ 1 cm² and indexed AVA ≤ 0.6 cm²/m², and stroke volume index ≤ 35 mL/m².

Multidetector computed tomography

Contrast-enhanced MDCT scans were performed using a dual-source computed tomography (CT) scanner (SOMATOM Force, Siemens Healthcare GmbH, Erlangen, Germany) with prospective electrocardiogram (ECG) triggering. CT angiography was performed with bolus tracking in the descending aorta using an 80 mL contrast agent bolus (Imeron 350, Bracco Imaging, Konstanz, Germany) at a flow rate of 4 mL/s, followed by a 40 mL saline chaser at the same flow rate. The following scan parameters were used: $2 \times 192 \times 0.6$ mm collimation, 250 ms rotation time, pitch of 3.2, and automated tube current adaption. A small field of view data set with medium soft convolution kernel (Siemens Bv36) and 0.75 mm slice thickness was generated for the assessment of the aortic annulus, root, valve morphology, and dimensions. Structures relevant for TAVR planning were assessed as recommended by current expert consensus.¹³ All data were analysed using a dedicated software (3mensio Structural Heart V9.1, Pie Medical Imaging, Maastricht, the Netherlands).¹⁴ As previously recommended, an individual threshold of the Hounsfield

Figure 1 Characterization of the study population. AS, aortic stenosis; LEFHG, low ejection fraction high-gradient; LEFLG, low ejection fraction low-gradient; NEFHG, normal ejection fraction high-gradient; PLFLG, paradoxical low-flow, low-gradient.



units (HU) was used to distinguish between calcium and contrast medium.^{8,15} An empirical threshold of 550 HU was used and adjusted as appropriate according to Ludwig *et al.*⁸ AVC was defined as calcification within the valve leaflets, aortic annulus, or aortic wall up to the sinotubular junction.⁸ The calcification of the coronary arteries was excluded from the region of interest (see *Figure 2*). Calcium score was expressed as mm³.^{3,16}

Transfemoral transcatheter aortic valve replacement

TAVR was performed at the TAVR centre of the University Medical Center Göttingen, which is certified according to quality requirements of the German Society of Cardiology.¹⁷

In most of the study participants, an Edwards SAPIEN 3™ (90%) or a Medtronic CoreValve (7%) prosthesis was implanted.

Assessment of myocardial fibrosis using endomyocardial biopsies

Following TAVR, five LV biopsies were taken from the basal anterior septum using a biopsy forceps (Proflex-Bioptom 7F, Medical Imaging Systems) by an interventional cardiologist.

The biopsies were fixed in 10% paraformaldehyde and embedded in paraffin. MF was assessed blinded to clinical and imaging data using quantitative morphometry (Olympus software cellSens 1.6) and defined as blue area in Masson's trichrome-stained biopsy sections (section with positive staining for collagen) in relation to total tissue area. The analyses were performed by a molecular cardiologist.

Statistical analysis

Statistical analyses were performed using IBM SPSS Statistics Version 26 for Windows [International Business Machines Corporation (IBM® Corp.), Armonk, NY, USA]. Data are expressed as mean ± standard deviations. Normal distribution was tested using the Shapiro–Wilk test. Non-normally distributed data were compared using Mann–Whitney *U* and Kruskal–Wallis tests as appropriate. For between-group comparisons in normally distributed data, *t*-test or ANOVA test was performed as appropriate. *Post hoc* analyses were carried out using the Bonferroni correction. For binary variables, the intergroup comparison was done using the χ^2 test. For intragroup comparisons, each AS subtype was divided by the group-specific AVC median. Survival analyses were performed by comparing the procedure (TAVR) with event time for mortality and CV mortality using Kaplan–Meier plots,

Figure 2 Calcium quantification on contrast-enhanced multidetector computed tomography (MDCT) images. (A) Region of interest measuring aortic valve calcification (AVC). (B) Region of interest measuring the calcification of the device landing zone (DLZ) [AVC area and left ventricular outflow tract (LVOT) area]. (C) Quantification within the AVC according to the left coronary cusp (LC), right coronary cusp (RC), and non-coronary cusp (NC).

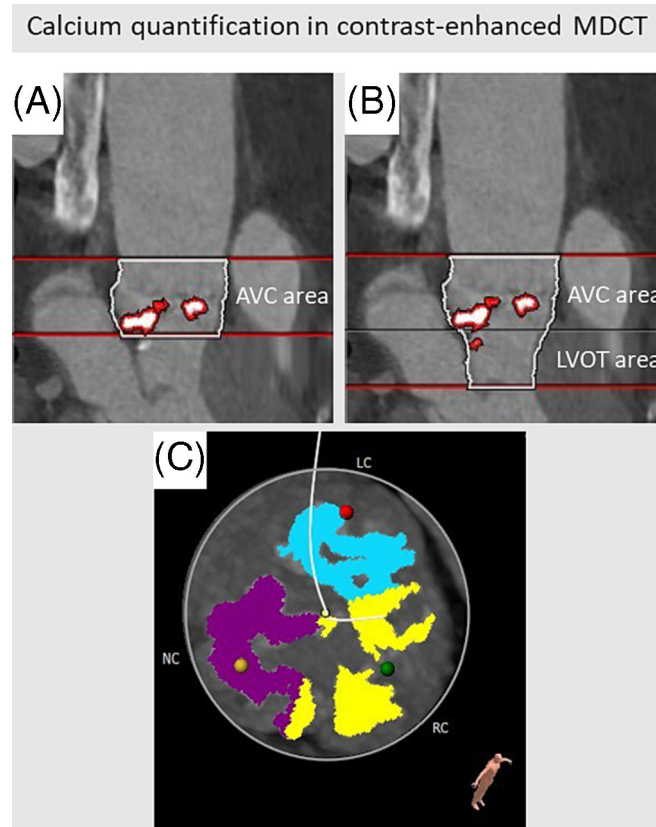


Table 1 Patients' characteristics

	All patients	NEFHG	LEFHG
Patients, <i>n</i> (%)	92 (100)	39 (42.4)	13 (14.1)
Age (years)	79 ± 7 (57–92)	78 ± 7 (57–92)	78 ± 9 (62–90)
Female, <i>n</i> (%)	33 (35.9)	15 (38.5)	5 (38.5)
BMI (kg/m ²)	28.29 ± 5.40 (19.03–45.91)	28.48 ± 5.76 (19.03–42.25)	29.38 ± 6.56 (20.78–45.91)
BSA (m ²)	1.93 ± 0.23 (1.45–2.71)	1.92 ± 0.23 (1.6–2.71)	1.97 ± 0.27 (1.61–2.46)
AVC (mm ³)	683.8 ± 432.7 (25.9–2406.4)	806.6 ± 421.3 (144–1770.9)	812.6 ± 281.4 (376.1–1353.3)
Fibrosis (%)	20.2 ± 21.3 (0–88)	13.7 ± 16.2 (1–67)	27.1 ± 23.5 (1–81)
Hypertension, <i>n</i> (%)	89 (96.7)	38 (97.4)	11 (54.6)
Atrial fibrillation, <i>n</i> (%)	41 (44.6)	16 (41)	4 (30.8)
Coronary artery disease, <i>n</i> (%)	64 (69.6)	25 (64.1)	8 (61.5)
Stroke, <i>n</i> (%)	13 (14.1)	5 (12.8)	1 (7.7)
COPD, <i>n</i> (%)	17 (18.5)	6 (15.4)	1 (7.7)
Diabetes, <i>n</i> (%)	41 (44.6)	17 (43.6)	3 (23.1)
NYHA	2.85 ± 0.74 (1–4)	2.59 ± 0.79 (1–4)	2.92 ± 0.76 (2–4)
6MWT (m)	206 ± 117 (0–401)	248 ± 94 (0–401)	163 ± 116 (0–401)
NT-proBNP (ng/l)	5211 ± 9795 (84.8–70 000)	2264 ± 3445 (84.8–15 016)	10 663 ± 11 416 (1913–38 807)

6MWT, 6 min walk test; AVC, aortic valve calcification; BMI, body mass index; BSA, body surface area; COPD, chronic obstructive pulmonary disease; LEFHG, low ejection fraction high-gradient; LEFLG, low ejection fraction low-gradient; NEFHG, normal ejection fraction high-gradient; NT-proBNP, N-terminal pro-B-type natriuretic peptide; NYHA, New York Heart Association; PLFLG, paradoxical low-flow, low-gradient.

Values are given for all patients and also separated into the different aortic stenosis subtypes. Significant differences are indicated by *P* values in bold. Data are expressed as absolute numbers, percentage, or mean ± standard deviation and minimum–maximum.

and significance was calculated using the log-rank test. A *P* value below 0.05 was considered statistically significant. Intra- and inter-observer variability was derived from a repeated measurement after at least 4 weeks in a subset of 10 randomly selected patients. The analysis of a second skilled observer was used to assess inter-observer reproducibility. Intra- and inter-observer variability was quantified using the intraclass correlation coefficient (ICC) reliability method, Bland–Altman analysis, and coefficient of variation (CoV).¹⁸ CoV was defined as the standard deviation of the differences divided by the mean.¹⁹ ICC reliability was scored as excellent (>0.74), good (0.6–0.74), fair (0.4–0.59), and poor (<0.4) as previously defined.²⁰

Results

Patients' characteristics

The mean age of our patient cohort was 79 ± 7 years, and 33 (35.9%) patients were female. The body mass index (BMI) was slightly elevated (28.3 ± 5.4 kg/m²) according to the World Health Organization (WHO) definition.²¹ The most common CV comorbidities were hypertension (96.7%), coronary artery disease (69.6%), and atrial fibrillation (AF) (44.6%). A total of 44.6% of the patients were also suffering from diabetes mellitus (DM) and 18.5% from chronic obstructive pulmonary disease (COPD).

Patients were classified according to AS subtypes: NEFHG AS 39 (42.4%), LEFHG AS 13 (14.1%), LEFLG 25 (27.2%), and PLFLG AS 15 (16.3%).

A summary of the patients' characteristics is illustrated in *Table 1*.

Echocardiography

Echocardiographic results are presented in *Table 2* as well as in Supporting Information, *Table S1*. Comparison of the AS subgroups shows that LV end-diastolic (LVEDV) and end-systolic volumes (LVESV) were significantly enlarged in the subgroups with reduced EF (*P* < 0.001). These two subgroups also had a numerically increased LV muscle index (LVMI) compared with the subgroups with normal EF, with statistically significant differences between the LEFHG and PLFLG AS subtypes (*P* = 0.005). The right ventricular (RV) function, measured by tricuspid annular plane systolic excursion (TAPSE), was in normal range for all subgroups and lowest in the low-gradient phenotypes. Significant differences were observed between NEFHG AS and the low-gradient subtypes (LEFLG AS, *P* = 0.002; PLFLG AS, *P* = 0.01).

Multidetector computed tomography

Mean aortic annulus area of 562.3 ± 98.4 mm², LV outflow tract (LVOT) area of 507 ± 100.8 mm², and the ascending aorta area of 928.1 ± 183.1 mm² were calculated. All measurements were performed using an individual HU threshold of 547.2 ± 84.3 . The mean AVC score was 683.8 ± 432.7 mm³. For the overall cohort, the non-coronary cusp showed the largest amount of calcification, followed by left coronary and right coronary cusps. Although, these patterns were also

Table 1 (continued)

	LEFLG	PLFLG	<i>P</i> value
Patients, <i>n</i> (%)	25 (27.2)	15 (16.3)	
Age (years)	79 ± 6 (66–90)	81 ± 5 (68–89)	<i>P</i> = 0.483
Female, <i>n</i> (%)	5 (20)	8 (53.3)	<i>P</i> = 0.181
BMI (kg/m ²)	28.19 ± 5.37 (20.59–41.40)	27.04 ± 3.24 (23–33.33)	<i>P</i> = 0.883
BSA (m ²)	1.92 ± 0.22 (1.53–2.45)	1.91 ± 0.22 (1.45–2.26)	<i>P</i> = 0.938
AVC (mm ³)	502.5 ± 325.6 (25.9–1295.2)	555.4 ± 593.6 (80.7–2406.4)	<i>P</i> = 0.001
Fibrosis (%)	29.1 ± 26.9 (0–88)	16.4 ± 14.1 (0–45)	<i>P</i> = 0.045
Hypertension, <i>n</i> (%)	25 (100)	15 (100)	<i>P</i> = 0.058
Atrial fibrillation, <i>n</i> (%)	10 (40.0)	11 (73.3)	<i>P</i> = 0.092
Coronary artery disease, <i>n</i> (%)	20 (80.0)	11 (73.3)	<i>P</i> = 0.506
Stroke, <i>n</i> (%)	5 (20)	2 (13.3)	<i>P</i> = 0.749
COPD, <i>n</i> (%)	7 (28)	3 (20)	<i>P</i> = 0.427
Diabetes, <i>n</i> (%)	13 (52)	8 (53.3)	<i>P</i> = 0.325
NYHA	3.16 ± 0.55 (2–4)	2.93 ± 0.70 (1–4)	<i>P</i> = 0.105
6MWT (m)	179 ± 113 (0–361)	180 ± 120 (0–388)	<i>P</i> = 0.054
NT-proBNP (ng/l)	$8547 \pm 14\,976$ (262.6–70\,000)	2193 ± 1212 (777.8–3966)	<i>P</i> < 0.001

6MWT, 6 min walk test; AVC, aortic valve calcification; BMI, body mass index; BSA, body surface area; COPD, chronic obstructive pulmonary disease; LEFHG, low ejection fraction high-gradient; LEFLG, low ejection fraction low-gradient; NEFHG, normal ejection fraction high-gradient; NT-proBNP, N-terminal pro-B-type natriuretic peptide; NYHA, New York Heart Association; PLFLG, paradoxical low-flow, low-gradient.

Values are given for all patients and also separated into the different aortic stenosis subtypes. Significant differences are indicated by *P* values in bold. Data are expressed as absolute numbers, percentage, or mean \pm standard deviation and minimum–maximum.

Table 2 Echocardiographic findings for all patients and separated by the different aortic stenosis subtypes

	All patients	NEFHG	LEFHG	LEFLG	PLFLG	P value
Patients, n (%)	92 (100)	39 (42.4)	13 (14.1)	25 (27.2)	15 (16.3)	
EF (%)	49.6 ± 15.3 (17–75)	61.2 ± 5.5 (50.4–75)	32.9 ± 10.6 (17–47)	34.6 ± 9.7 (17.1–48)	59.1 ± 7.4 (50–74.4)	P < 0.001
LVEDV (mL)	94 ± 42 (25–222)	77 ± 32 (32.3–184)	131 ± 44 (76–203)	117 ± 35 (70–222)	67 ± 33 (25–151)	P < 0.001
LVESV (mL)	52 ± 36 (11–184)	30 ± 14 (11.2–75)	90 ± 41 (44–166)	78 ± 33 (37–184)	28 ± 16 (11–74.9)	P < 0.001
V _{max} (m/s)	3.92 ± 0.75 (2.48–6.3)	4.47 ± 0.49 (4.0–6.3)	4.38 ± 0.51 (4.0–5.99)	3.23 ± 0.41 (2.48–3.94)	3.24 ± 0.32 (2.63–3.74)	P < 0.001
P _{mean} (mmHg)	37.7 ± 16.0 (12–108)	49.0 ± 14.0 (35–108)	45.4 ± 11.0 (31–79)	23.9 ± 6.2 (12–35)	24.7 ± 5.5 (16–33)	P < 0.001
AVA (cm ²)	0.73 ± 0.17 (0.4–1.2)	0.73 ± 0.18 (0.4–1.2)	0.61 ± 0.12 (0.4–0.8)	0.76 ± 0.18 (0.45–1.1)	0.78 ± 0.13 (0.5–1.0)	P = 0.038
ΔAV P _{mean} (mmHg)	27.3 ± 14.6 (3–92)	37.9 ± 13.3 (14–92)	33.2 ± 8.4 (23–56)	16.1 ± 7.2 (3–30)	14.7 ± 5.9 (5–28)	P < 0.001
at discharge						
TAPSE (mm) (n = 84)	20.5 ± 4.7 (11–33)	22.9 ± 4.6 (11–33)	19.6 ± 3.5 (14–25)	18.4 ± 4.2 (11–28)	18.6 ± 4.0 (12–26)	P = 0.001

AV, aortic valve; AVA, aortic valve area; EF, ejection fraction; LEFHG, low ejection fraction high-gradient; LEFLG, low ejection fraction low-gradient; LVEDV, left ventricular end-diastolic volume; LVESV, left ventricular end-systolic volume; NEFHG, normal ejection fraction high-gradient; PLFLG, paradoxical low-flow, low-gradient; TAPSE, tricuspid annular plane systolic excursion.

Significant differences are indicated by *P* values in bold.

found in the high-gradient AS subtypes, no clear distribution pattern was observed in the low-gradient subtypes.

AVC correlated with the transvalvular gradient and was larger in high-gradient AS [NEFHG (806.6 ± 421.3 mm³) and LEFHG (812.6 ± 281.1 mm³)] compared with the low-gradient subtypes [LEFLG (502.5 ± 325.6 mm³) and PLFLG (555.4 ± 593.6 mm³), *P* = 0.01] (Figures 3 and 4). LVOT calcification was significantly larger in the NEFHG AS subgroup (126.9 ± 158.5 mm³) compared with the low-gradient subtypes [LEFLG (29.4 ± 45.4 mm³), *P* = 0.004; PLFLG (65.4 ± 110.1 mm³), *P* = 0.015], but not compared with LEFHG (55.1 ± 77.6 mm³, *P* = 0.108).

Intragroup and intergroup comparison of aortic stenosis subtypes using aortic valve calcification

Dividing the AS subgroups by their specific intragroup median calcium scores revealed no differences in terms of age, sex, BMI, as well as the amount of MF for the NEFHG, LEFHG, and PLFLG. However, significant differences were found in the LEFLG subgroup: more female patients were in the group, and the intragroup-specific calcium burden was below the median (*P* = 0.009). In contrast, the degree of MF was significantly higher in patients with a more calcified AS (>median) (*P* = 0.027).

Although there were no differences in echocardiographic findings in LEFHG and PLFLG AS, the mean aortic gradient was significantly increased in patients with larger AVC in the NEFHG (54.2 ± 16.3 vs. 43.4 ± 8.2 mmHg, *P* = 0.014) and LEFLG (26.7 ± 5.1 vs. 20.8 ± 6.0 mmHg, *P* = 0.014) subtypes.

MDCT measurements revealed no significant differences for any of the measured parameters in the intragroup comparison (AVC ≥ median or <median) of the normal EF subtypes. In the low EF subtypes, higher amounts of calcium were associated with larger aortic annulus areas.

Histology

The average extent of MF was 20.2 ± 21.3%. Comparison of the AS subtypes showed the lowest amount of MF in the NEFHG group (13.7 ± 16.2%) followed by the PLFLG group (16.4 ± 14.1%). The largest amount was measured in the LEFLG group (29.1 ± 26.9%). Statistically significant differences were observed between the NEFHG subtype and the EF subtypes (LEFHG, *P* = 0.03; LEFLG, *P* = 0.02).

Cardiovascular events

In total, 22 patients died within the follow-up after TAVR. Among these, 14 deaths were characterized as CV deaths. Comparing survivors with patients dying from CV causes

Figure 3 Diagram of the relationship between aortic valve calcification (AVC) and transaortic valve gradient expressed as mean gradient (P_{mean}).

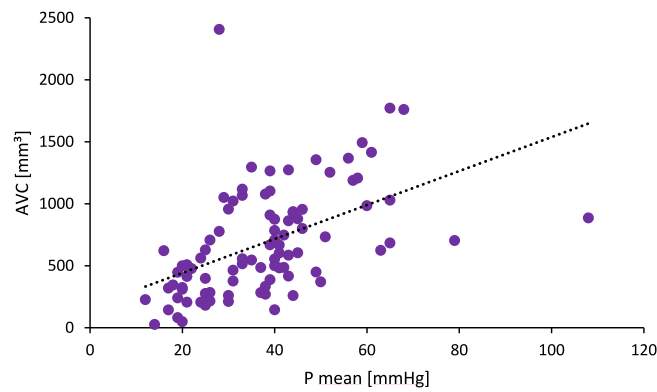
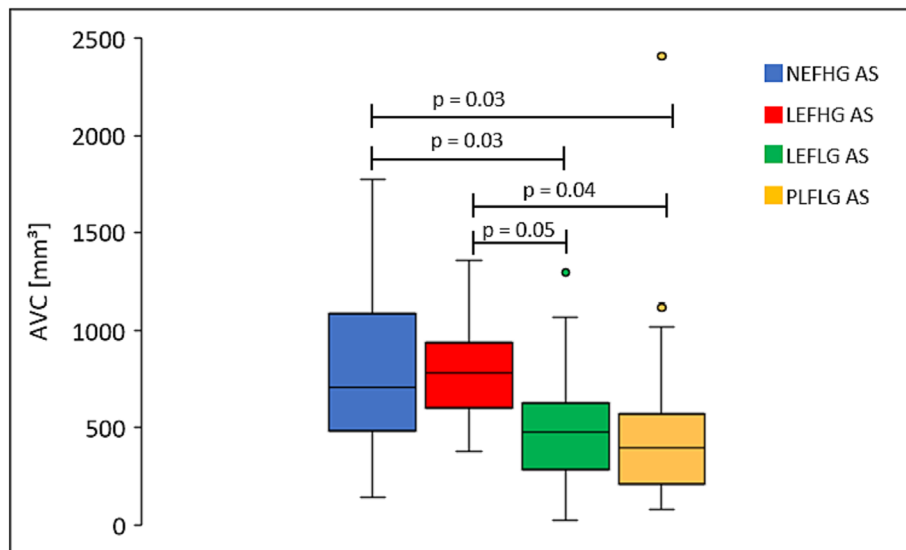


Figure 4 Aortic valve calcification (AVC) distribution according to the aortic stenosis (AS) subtypes by echocardiography. Significant differences using Kruskal–Wallis test and Bonferroni correction are labelled. LEFHG, low ejection fraction high-gradient; LEFLG, low ejection fraction low-gradient; NEFHG, normal ejection fraction high-gradient; PLFLG, paradoxical low-flow, low-gradient.



shows significant differences in terms of MF ($P = 0.004$), New York Heart Association (NYHA) class ($P = 0.04$), 6MWT ($P = 0.009$), and the presence of AF ($P = 0.028$) and DM ($P = 0.001$). No differences were seen regarding age, sex, BMI, and N-terminal pro-B-type natriuretic peptide (NT-proBNP) (Table 3). Furthermore, significant differences in mortality rates were observed between the AS subgroups (NEFHG AS 2.5%; LEFHG AS 15.4%; PLFLG AS 26.7%; and LEFLG AS 28%; $P = 0.023$). Interestingly, the survivors showed a higher AVC compared with the deceased, although this difference did not reach statistical significance ($P = 0.088$). In the group of patients with a high MF burden, patients with a high AVC showed a significantly higher survival rate follow-

ing TAVR [hazard ratio (HR) 0.261; 95% confidence interval (CI) 0.07–0.97; $P = 0.045$] (Figure 5).

Intra-observer and inter-observer agreement and reproducibility

The agreement and reproducibility of the data were excellent. The results of the intra- and inter-observer agreement and reproducibility test are shown in Supporting Information, Table S2. Bland–Altman plots are displayed in Supporting Information, Figure S1.

Table 3 Illustration of the baseline characteristics separated for survivors and CV deaths

	All patients	Survivor	CV deaths	P value
Patients (%)	92	78	14	
Age (years)	79 ± 7 (57–92)	79 ± 7 (57–92)	76 ± 7 (62–88)	<i>P</i> = 0.172
Sex (female), <i>n</i> (%)	33 (35.9)	29 (37.2)	4 (28.6)	<i>P</i> = 0.568
BMI (kg/m ²)	28.3 ± 5.4 (19.0–45.9)	27.9 ± 4.9 (19.0–42.3)	30.6 ± 7.6 (22.5–45.9)	<i>P</i> = 0.221
BSA (m ²)	1.93 ± 0.23 (1.45–2.71)	1.90 ± 0.21 (1.45–2.71)	2.04 ± 0.27 (1.59–2.46)	<i>P</i> = 0.059
AVC (mm ³)	683.8 ± 432.7 (25.9–2406.4)	719.6 ± 450.5 (25.9–2406.4)	484.7 ± 241.9 (80.7–1021.2)	<i>P</i> = 0.088
AVC/area (mm ³ /mm ²)	1.21 ± 0.75 (0.07–4.13)	1.27 ± 0.78 (0.07–4.13)	0.88 ± 0.41 (0.15–1.64)	<i>P</i> = 0.062
Fibrosis (%)	20.2 ± 21.3 (0–88)	17.9 ± 20.1 (0–84)	33.4 ± 23.7 (2–88)	<i>P</i> = 0.004
Hypertension, <i>n</i> (%)	89 (96.7)	75 (96.2)	14 (100)	<i>P</i> = 0.456
Atrial fibrillation, <i>n</i> (%)	41 (44.6)	31 (39.7)	10 (71.4)	<i>P</i> = 0.028
Coronary artery disease, <i>n</i> (%)	64 (69.6)	54 (69.2)	10 (71.4)	<i>P</i> = 0.869
Stroke, <i>n</i> (%)	13 (14.1)	11 (14.1)	2 (14.3)	<i>P</i> = 0.986
COPD, <i>n</i> (%)	17 (18.5)	15 (19.2)	2 (14.3)	<i>P</i> = 0.661
Diabetes, <i>n</i> (%)	41 (44.6)	29 (37.2)	12 (85.7)	<i>P</i> = 0.001
NYHA	2.85 ± 0.74 (1–4)	2.78 ± 0.77 (1–4)	3.21 ± 0.43 (3–4)	<i>P</i> = 0.04
6MWT (m)	206 ± 117 (0–401)	218 ± 115 (0–401)	124 ± 96 (0–325)	<i>P</i> = 0.009
NT-proBNP (ng/l)	5211 ± 9795 (84.8–70 000)	4326 ± 6496 (84.8–38 807)	9636 ± 19 106 (262.6–70 000)	<i>P</i> = 0.324

6MWT, 6 min walk test; AVC, aortic valve calcification; BMI, body mass index; BSA, body surface area; COPD, chronic obstructive pulmonary disease; CV, cardiovascular; NT-proBNP, N-terminal pro-B-type natriuretic peptide; NYHA, New York Heart Association. Significant differences are indicated by *P* values in bold.

Discussion

This is the first study to comprehensively characterize a large cohort of AS patients with echocardiography, invasive LV biopsies, and MDCT imaging.

The following notable findings were observed: first, calcium load and distribution discriminate between different haemodynamic subtypes of AS. Second, low-flow situations are associated with larger amounts of MF, higher CV mortality, but lower amounts of calcium. Among patients with LEFLG AS and presence of relatively large amounts of MF, MDCT calcium scoring allows further discrimination of patients at high risk of CV mortality following TAVR. Third, in the presence of large MF burden, patients with large calcium load have better outcome following TAVR. Conversely, worse outcome associated with large MF and relatively little calcium load may be explained by a relative prominence of an underlying cardiomyopathy, whereas better survival rates in large calcium load situations may indicate severe AS-associated pressure overload relief and subsequently improved survival following TAVR. Fourth, higher mortality rates were seen in low-gradient AS phenotypes compared with the high-gradient phenotypes. Finally, calcium load is well detectable using contrast-enhanced MDCT and can be quantified on routinely acquired pre-TAVR MDCT contrast-enhanced images.

Phenotypes of aortic stenosis: calcium load, calcium distribution, and myocardial fibrosis

MDCT scans are widely used in clinical routine for different indications. Although the European Society of Cardiology

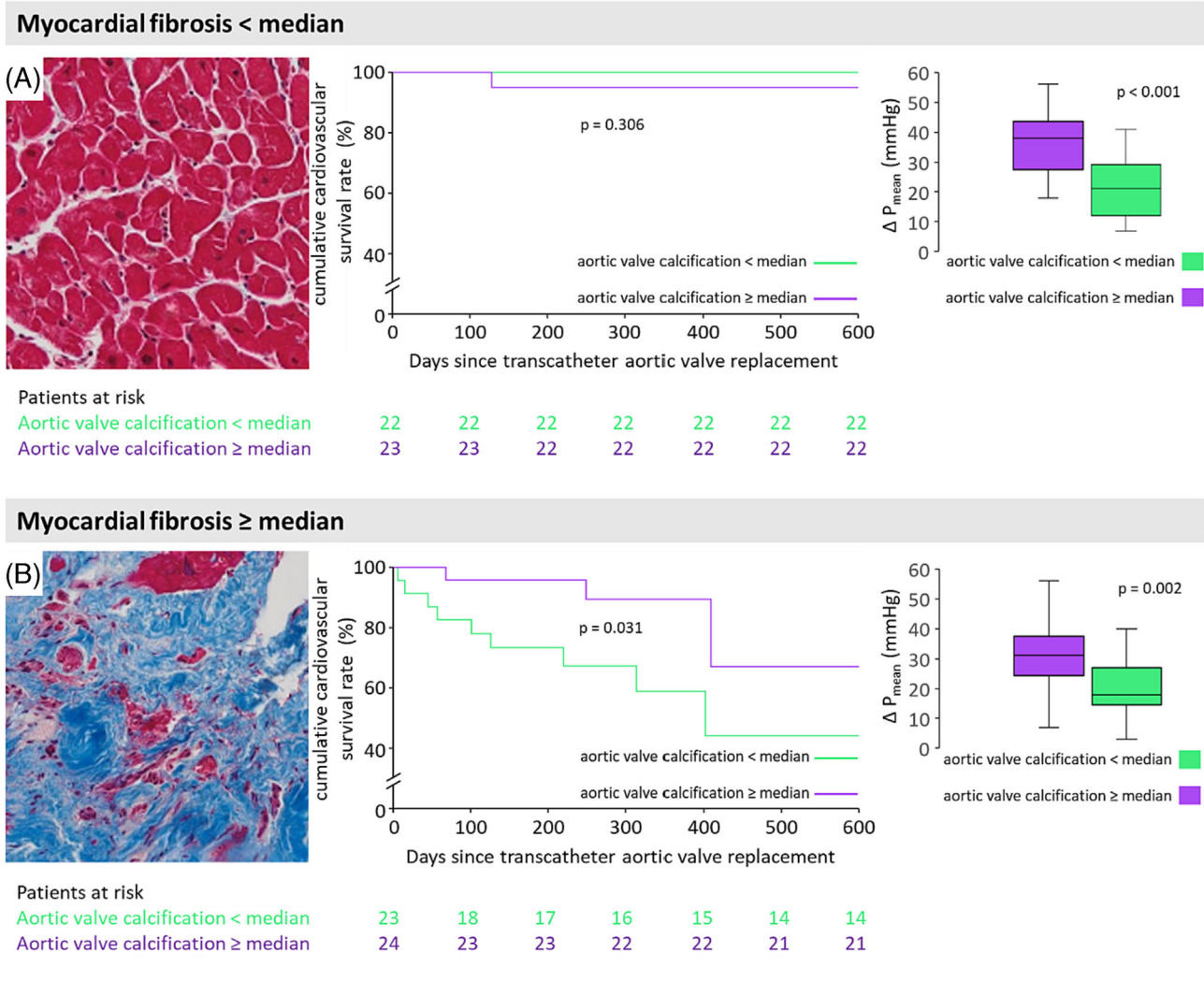
(ESC) guidelines refer to the diagnostic importance of MDCT in patients with AS without a high-gradient situation, contrast-enhanced MDCT is also important in the selection of the patient-specific valve prosthesis.¹³

Furthermore, different studies have shown the correlation between the severity of AS and AVC.^{3,22} A correlation between high calcium burden and higher transaortic valve gradients was also observed in our study for all subtypes of AS.

In concordance with the findings of Seiffert *et al.*, in the overall cohort, the most calcified cusp was the non-coronary cusp followed by the left coronary and right coronary cusps.¹⁵ These findings are also reproducible in the subgroup of high-gradient AS. Dweck *et al.* reported this characteristic distribution as a result of an increased mechanical and a reduced shear stress.²³ The 'protective' shear stress is lowest in the non-coronary cusp, which results in predominant calcification and very frequent contribution of this cusp to AS development.²³ In our study, patients with low-gradient AS did not demonstrate a clear distribution pattern of calcification in the different cusps. This finding could be directly attributable to low-flow situations, which result in lower mechanical stress. In the NEFHG subtype, in addition to the distribution of the calcium load in relation to the various cusps, a significantly higher calcium load was present in the LVOT compared with low ejection/flow phenotypes (LEFHG, LEFLG, and PLFLG).

The different calcium distribution phenotypes of the aortic valve in the different AS subtypes, with the lowest calcium found in the low EF groups, could be an indirect indication that these subgroups represent different entities rather than a continuum of disease. It is interesting to speculate that there may not be a common transition between groups and that potentially, the sub-division into groups may occur at a

Figure 5 Cardiovascular mortality depending on aortic valve calcification in patients with myocardial fibrosis (A) below median and (B) above median. The box plots in the upper right side indicate the pressure relief following transcatheter aortic valve replacement (TAVR), depending on the aortic valve calcification.



very early disease stage. The amount of calcification in LEFLG AS could help to identify the role of the AS in the impairment of LV function. In patients with AS with a ‘typical high load’ calcium pattern in the presence of a low-flow, low-gradient situation, the calcium distribution could be indicative of valve-associated deterioration of LV function. In contrast, an unspecific calcium distribution may indicate LV dysfunction that preceded the AS development or occurred very early during AS development without formation of larger calcium amounts during constant high-pressure exposure.

With regard to MF, the highest proportion was found in the low EF subtypes. A similar observation was reported by Rosa *et al.*, whose magnetic resonance imaging (MRI) findings showed that MF was significantly higher in LEFLG AS compared with the classical NEFHG AS.²⁴ Because increased MF is known to be associated with delayed normalization of LV

geometry as well as function following TAVR, the determination of the calcium load in the LEFLG group could possibly provide indications for therapeutic responses in these patients.¹⁰

Clinical significance and implications for mortality

Several studies have demonstrated that low-gradient AS, especially combined with reduced EF and low flow, is associated with a worse prognosis after TAVR as compared with other AS subtypes.^{25–27} However, the true survival rate in TAVR patients with PLFLG AS remains unclear. Some studies reported comparable outcomes to NEFHG AS, but others demonstrated worse outcome in PLFLG AS patients.^{25–27} In our study, the highest mortality rates were observed in patients with LEFLG AS, followed by patients with PLFLG AS.

Some observational studies have described an association between AVC and mortality also in patients with severe AS who did not undergo a surgical or interventional treatment. There is also some evidence suggesting that in patients undergoing aortic valve replacement, higher amounts of AVC are associated with better survival rates.⁵ It is interesting that the amount of AVC did not solely predict survival rates in our cohort.

Furthermore, no relationship between AVC and mortality could be documented in the AS subgroups neither, which may be explained by the relatively small sample size and event rate. However, taking MF into account, AVC became an important additional predictor of poor survival rates in AS. MF can be divided into two patterns: reactive interstitial fibrosis that occurs in the early stages of AS and is potentially reversible and replacement fibrosis.²⁸ Regardless of the pattern, the presence of MF is known to be associated with poor long-term outcomes in different CV conditions.^{9,10,29–36} There is also increasing evidence pointing to the pathophysiological role of MF in AS. With histological data, Puls *et al.* demonstrated that MF burden differed significantly between AS subtypes, with the highest amount found in the LEFLG AS subtype.¹⁰ From a functional standpoint, MF results in reduced LV function and the occurrence of heart failure symptoms. In addition, an increased MF load was associated with a delayed normalization of LV geometry and LV function and also associated with a higher CV mortality, most likely due to arrhythmogenic potential in patients who underwent TAVR.¹⁰ Using MRI non-invasive measurements, Everett *et al.* have shown that the extracellular volume fraction as a marker of fibrosis can serve as an independent predictor of mortality in AS patients.⁹ In our patients with large MF burden, those with high AVC had a better survival compared with those with low AVC. These findings are in concordance with the results of Ludwig *et al.* who found that high calcium loads in LEFLG AS were a predictor of lower mortality following TAVR.⁸ The authors justified this with the fact that in patients with a high amount of calcium, the crucial pathogen is eliminated by the TAVR procedure, whereas in patients with a lower amount of calcium, the comorbidities may be decisive for the prognosis, and the AS may be of less importance.

Limitations

Several limitations need to be considered. First, this is a single-centre study and our findings need to be reproduced by other sites. Second, AVC was estimated on contrast-enhanced MDCT only and not on native calcium scoring scans. Due to the contrast-enhanced MDCT used, threshold adjustment can be necessary to discriminate between calcium and intraluminal contrast medium, which can lead to difficulties in reproducibility. However, in our study, intra- and inter-observer reliability was excellent,

which is in line with previous publications.¹⁶ Therefore, we believe that contrast-enhanced MDCT is sufficient to estimate AVC and could be a useful addendum to routine clinical practice. Third, CV mortality has been defined according to the VARC definition. Although this definition is widely accepted, it is important to note that sudden/unwitnessed deaths of unknown causes are also registered as CV mortalities. Although 13 of the 14 deaths in our patient cohort were documented as definitively due to CV causes, one patient's death was an unexpected sudden death and was therefore, according to the VARC definition, included in the reported CV-related mortality. Fourth, because only 100 patients were consecutively enrolled, the subtype groups are of different sizes, which has implications for statistical testing. However, our study still demonstrates a respective contribution of AVC and MF on CV mortality. Fifth, myocardial biopsies were used to assess MF. Although histological assessments offer in-depth tissue characterization, sampling errors may occur. However, cardiac magnetic resonance scans as an alternative also are accompanied by advantages and disadvantages such as software-specific native T1 times and differing normal values.³⁷ Furthermore, in the absence of follow-up examinations, we are unable to report on reverse remodelling in regard to AVC and MF.³⁸ Finally, our study included Medtronic CoreValve and the Edwards SAPIEN 3™ valves, which were standard devices at the time of data collection.

Conclusions

MF is associated with adverse CV outcome following TAVR, which is most prevalent in low EF situations. In the presence of large MF burden, patients with large AVC have better outcome following TAVR. Conversely, worse outcome in large MF and relatively little AVC may be explained by a relative prominence of an underlying cardiomyopathy. Finally, better survival rates in patients with large AVC may be indicative of severe AS-associated pressure overload relief and subsequently improved survival following TAVR.

Acknowledgements

We acknowledge support by the open Access Publication Funds of the Göttingen University. Open Access funding enabled and organized by Projekt DEAL. [Correction added on 26 April 2023, after first online publication: Acknowledgements section has been added in this version.]

Conflict of interest

None declared.

Funding

The study was funded by a grant from the German Research Foundation [Deutsche Forschungsgemeinschaft (DFG, CRC 1002, D1)].

Supporting information

Additional supporting information may be found online in the Supporting Information section at the end of the article.

References

- Vahanian A, Praz F, Milojevic M, Beyersdorf F. 2021 ESC/EACTS guidelines for the management of valvular heart disease. *Eur Heart J*. 2021; **42**: 4207–4208.
- Iung B, Baron G, Butchart EG, Delahaye F, Gohlke-Bärwolf C, Levang OW, Tornos P, Vanoverschelde JL, Vermeer F, Boersma E, Ravaut P, Vahanian A. A prospective survey of patients with valvular heart disease in Europe: the Euro Heart Survey on Valvular Heart Disease. *Eur Heart J*. 2003; **24**: 1231–1243.
- Cueff C, Serfaty JM, Cimadevilla C, Laissy JP, Humbert D, Tubach F, Duval X, Iung B, Enriquez-Sarano M, Vahanian A, Messika-Zeitoun D. Measurement of aortic valve calcification using multislice computed tomography: correlation with haemodynamic severity of aortic stenosis and clinical implication for patients with low ejection fraction. *Heart*. 2011; **97**: 721–726.
- Pawade T, Clavel MA, Tribouilloy C, Dreyfus J, Mathieu T, Tastet L, Renard C, Gun M, Jenkins WSA, Macron L, Sechrist JW, Lacomis JM, Nguyen V, Galian Gay L, Cuéllar Calabria H, Ntalas I, Cartlidge TRG, Prendergast B, Rajani R, Evangelista A, Cavalcante JL, Newby DE, Pibarot P, Messika Zeitoun D, Dweck MR. Computed tomography aortic valve calcium scoring in patients with aortic stenosis. *Circ Cardiovasc Imaging*. 2018; **11**: e007146.
- Clavel MA, Pibarot P, Messika-Zeitoun D, Capoulade R, Malouf J, Aggarwal SR, Araoz PA, Michelena HI, Cueff C, Larose E, Miller JD, Vahanian A, Enriquez-Sarano M. Impact of aortic valve calcification, as measured by MDCT, on survival in patients with aortic stenosis: results of an international registry study. *J Am Coll Cardiol*. 2014; **64**: 1202–1213.
- Wu VC, Takeuchi M, Nagata Y, Izumo M, Akashi YJ, Lin FC, Otsuji Y. Prognostic value of area of calcified aortic valve by 2-dimensional echocardiography in asymptomatic severe aortic stenosis patients with preserved left ventricular ejection fraction. *Medicine (Baltimore)*. 2018; **97**: e0246.
- Park JB, Hwang IC, Lee W, Han JK, Kim CH, Lee SP, Yang HM, Park EA, Kim HK, Chiam PTL, Kim YJ, Koo BK, Sohn DW, Ahn H, Kang JW, Park SJ, Kim HS. Quantified degree of eccentricity of aortic valve calcification predicts risk of paravalvular regurgitation and response to balloon post-dilation after self-expandable transcatheter aortic valve replacement. *Int J Cardiol*. 2018; **259**: 60–68.
- Ludwig S, Goßling A, Waldschmidt L, Linder M, Bhadra OD, Voigtländer L, Schäfer A, Deuschl F, Schirmer J, Reichenspurner H, Blankenberg S, Schäfer U, Westermann D, Seiffert M, Conradi L, Schofer N. TAVR for low-flow, low-gradient aortic stenosis: prognostic impact of aortic valve calcification. *Am Heart J*. 2020; **225**: 138–148.
- Everett RJ, Treibel TA, Fukui M, Lee H, Rigolli M, Singh A, Bijsterveld P, Tastet L, Musa TA, Dobson L, Chin C, Captur G, Om SY, Wiesemann S, Ferreira VM, Piechnik SK, Schulz-Menger J, Schelbert EB, Clavel MA, Newby DE, Myerson SG, Pibarot P, Lee S, Cavalcante JL, Lee SP, McCann GP, Greenwood JP, Moon JC, Dweck MR. Extracellular myocardial volume in patients with aortic stenosis. *J Am Coll Cardiol*. 2020; **75**: 304–316.
- Puls M, Beuthner BE, Topci R, Vogelgesang A, Bleckmann A, Sitte M, Lange T, Backhaus SJ, Schuster A, Seidler T, Kutschka I, Toischer K, Zeisberg EM, Jacobshagen C, Hasenfuß G. Impact of myocardial fibrosis on left ventricular remodelling, recovery, and outcome after transcatheter aortic valve implantation in different haemodynamic subtypes of severe aortic stenosis. *Eur Heart J*. 2020; **41**: 1903–1914.
- Beuthner BE, Topci R, Derks M, Franke T, Seelke S, Puls M, Schuster A, Toischer K, Valentova M, Cyganek L, Zeisberg EM, Jacobshagen C, Hasenfuß G, Nussbeck SY. Interdisciplinary research on aortic valve stenosis: a longitudinal collection of biospecimens and clinical data of patients undergoing transcatheter aortic valve replacement. *Open J Bioresour*. 2020; **7**: 3.
- VARC-3 Writing Committee, Généreux P, Piazza N, Alu MC, Nazif T, Hahn RT, Pibarot P, Bax JJ, Leipsic JA, Blanke P, Blackstone EH, Finn MT, Kapadia S, Linke A, Mack MJ, Makkar R, Mehran R, Popma JJ, Reardon M, Rodes-Cabau J, van Mieghem NM, Webb JG, Cohen DJ, Leon MB. Valve Academic Research Consortium 3: updated endpoint definitions for aortic valve clinical research. *J Am Coll Cardiol*. 2021; **77**: 2717–2746.
- Blanke P, Weir-McCall JR, Achenbach S, Delgado V, Hausleiter J, Jilaihawi H, Marwan M, Norgaard BL, Piazza N, Schoenhagen P, Leipsic JA. Computed tomography imaging in the context of transcatheter aortic valve implantation (TAVI)/transcatheter aortic valve replacement (TAVR): an expert consensus document of the Society of Cardiovascular Computed Tomography. *J Cardiovasc Comput Tomogr*. 2019; **13**: 1–20.
- Evertz R, Hub S, Kowallick JT, Seidler T, Danner BC, Hasenfuß G, Toischer K, Schuster A. Impact of observer experience on multi-detector computed tomography aortic valve morphology assessment and valve size selection for transcatheter aortic valve replacement. *Sci Rep*. 2022 Dec 12; **12**(1): 21430. <https://doi.org/10.1038/s41598-022-23936-w>. PMID: 36509862; PMCID: PMC9744877.
- Seiffert M, Fujita B, Avanesov M, Lunau C, Schön G, Conradi L, Prashovikj E, Scholtz S, Börgermann J, Scholtz W, Schäfer U, Lund G, Ensminger S, Treede H. Device landing zone calcification and its impact on residual regurgitation after transcatheter aortic valve implantation with different devices. *Eur Heart J Cardiovasc Imaging*. 2016; **17**: 576–584.

16. Evertz R, Hub S, Backhaus SJ, Lange T, Toischer K, Kowallick JT, Hasenfuß G, Schuster A. Head-to-head comparison of different software solutions for AVC quantification using contrast-enhanced MDCT. *J Clin Med*. 2021; **10**: 3970.
17. Kuck K-H, Eggebrecht H, Elsässer A, Hamm C, Haude M, Ince H, Katus H, Möllmann H, Naber CK, Schunkert H, Thiele H, Werner N. Qualitätskriterien zur Durchführung der kathetergestützten Aortenklappenimplantation (TAVI) Aktualisierung des Positionspapiers der Deutschen Gesellschaft für Kardiologie. *Kardiologe*. 2016; **10**: 282–300.
18. Bland JM, Altman DG. Statistical methods for assessing agreement between two methods of clinical measurement. *Lancet*. 1986; **1**: 307–310.
19. Morton G, Jogiya R, Plein S, Schuster A, Chiribiri A, Nagel E. Quantitative cardiovascular magnetic resonance perfusion imaging: inter-study reproducibility. *Eur Heart J Cardiovasc Imaging*. 2012; **13**: 954–960.
20. Oppo K, Leen E, Angerson WJ, Cooke TG, McArdle CS. Doppler perfusion index: an interobserver and intraobserver reproducibility study. *Radiology*. 1998; **208**: 453–457.
21. Arroyo-Johnson C, Mincey KD. Obesity epidemiology worldwide. *Gastroenterol Clin North Am*. 2016; **45**: 571–579.
22. Clavel MA, Messika-Zeitoun D, Pibarot P, Aggarwal SR, Malouf J, Araoz PA, Michelena HI, Cuffe C, Larose E, Capoulade R, Vahanian A, Enriquez-Sarano M. The complex nature of discordant severe calcified aortic valve disease grading: new insights from combined Doppler echocardiographic and computed tomographic study. *J Am Coll Cardiol*. 2013; **62**: 2329–2338.
23. Dweck MR, Boon NA, Newby DE. Calcific aortic stenosis: a disease of the valve and the myocardium. *J Am Coll Cardiol*. 2012; **60**: 1854–1863.
24. Rosa VEE, Ribeiro HB, Sampaio RO, Morais TC, Rosa MEE, Pires LJT, Vieira MLC, Mathias W Jr, Rochitte CE, de Santis ASAL, Fernandes JRC, Accorsi TAD, Pomerantzeff PMA, Rodés-Cabau J, Pibarot P, Tarasoutchi F. Myocardial fibrosis in classical low-flow, low-gradient aortic stenosis: insights from a cardiovascular magnetic resonance study. *Circ Cardiovasc Imaging*. 2019; **12**: e008353.
25. Puls M, Korte KP, Bleckmann A, Huenlich M, Danner B, Schoendube F, Hasenfuß G, Jacobshagen C, Schillinger W. Long-term outcomes after TAVI in patients with different types of aortic stenosis: the conundrum of low flow, low gradient and low ejection fraction. *EuroIntervention*. 2017; **13**: 286–293.
26. Fischer-Rasokat U, Renker M, Liebetrau C, van Linden A, Arsalan M, Weferling M, Rolf A, Doss M, Möllmann H, Walther T, Hamm CW, Kim WK. 1-year survival after TAVR of patients with low-flow, low-gradient and high-gradient aortic valve stenosis in matched study populations. *JACC Cardiovasc Interv*. 2019; **12**: 752–763.
27. Herrmann HC, Pibarot P, Hueter I, Gertz ZM, Stewart WJ, Kapadia S, Tuzcu EM, Babaliaros V, Thourani V, Szeto WY, Bavaria JE, Kodali S, Hahn RT, Williams M, Miller DC, Douglas PS, Leon MB. Predictors of mortality and outcomes of therapy in low-flow severe aortic stenosis: a Placement of Aortic Transcatheter Valves (PARTNER) trial analysis. *Circulation*. 2013; **127**: 2316–2326.
28. Treibel TA, Kozor R, Schofield R, Benedetti G, Fontana M, Bhuva AN, Sheikh A, López B, González A, Manisty C, Lloyd G, Kellman P, Díez J, Moon JC. Reverse myocardial remodeling following valve replacement in patients with aortic stenosis. *J Am Coll Cardiol*. 2018; **71**: 860–871.
29. Weng Z, Yao J, Chan RH, He J, Yang X, Zhou Y, He Y. Prognostic value of LGE-CMR in HCM: a meta-analysis. *JACC Cardiovasc Imaging*. 2016; **9**: 1392–1402.
30. Raina S, Lensing SY, Nairouz RS, Pothineni NV, Hakeem A, Bhatti S, Pandey T. Prognostic value of late gadolinium enhancement CMR in systemic amyloidosis. *JACC Cardiovasc Imaging*. 2016; **9**: 1267–1277.
31. Hulten E, Agarwal V, Cahill M, Cole G, Vita T, Parrish S, Bittencourt MS, Murthy VL, Kwong R, di Carli MF, Blankstein R. Presence of late gadolinium enhancement by cardiac magnetic resonance among patients with suspected cardiac sarcoidosis is associated with adverse cardiovascular prognosis: a systematic review and meta-analysis. *Circ Cardiovasc Imaging*. 2016; **9**: e005001.
32. di Marco A, Anguera I, Schmitt M, Klem I, Neilan TG, White JA, Sramko M, Masci PG, Barison A, McKenna P, Mordi I, Haugaa KH, Leyva F, Rodriguez Capitán J, Satoh H, Nabeta T, Dallaglio PD, Campbell NG, Sabaté X, Cequier A. Late gadolinium enhancement and the risk for ventricular arrhythmias or sudden death in dilated cardiomyopathy: systematic review and meta-analysis. *JACC Heart Fail*. 2017; **5**: 28–38.
33. Halliday BP, Gulati A, Ali A, Guha K, Newsome S, Arzanauskaitė M, Vassiliou VS, Lota A, Izgi C, Tayal U, Khalique Z, Stirrat C, Auger D, Pareek N, Ismail TF, Rosen SD, Vazir A, Alpendurada F, Gregson J, Frenneaux MP, Cowie MR, Cleland JGF, Cook SA, Pennell DJ, Prasad SK. Association between midwall late gadolinium enhancement and sudden cardiac death in patients with dilated cardiomyopathy and mild and moderate left ventricular systolic dysfunction. *Circulation*. 2017; **135**: 2106–2115.
34. Aquaro GD, Perfetti M, Camastra G, Monti L, Dellegrottaglie S, Moro C, Pepe A, Todiere G, Lanzillo C, Scatteia A, di Roma M, Pontone G, Perazzolo Marra M, Barison A, di Bella G. Cardiac MR with late gadolinium enhancement in acute myocarditis with preserved systolic function: ITAMY study. *J Am Coll Cardiol*. 2017; **70**: 1977–1987.
35. Ganesan AN, Gunton J, Nuficora G, McGavigan AD, Selvanayagam JB. Impact of late gadolinium enhancement on mortality, sudden death and major adverse cardiovascular events in ischemic and nonischemic cardiomyopathy: a systematic review and meta-analysis. *Int J Cardiol*. 2018; **254**: 230–237.
36. Becker MAJ, Cornel JH, van de Ven PM, van Rossum AC, Allaart CP, Germans T. The prognostic value of late gadolinium-enhanced cardiac magnetic resonance imaging in nonischemic dilated cardiomyopathy: a review and meta-analysis. *JACC Cardiovasc Imaging*. 2018; **11**: 1274–1284.
37. Backhaus SJ, Lange T, Beuthner BE, Topci R, Wang X, Kowallick JT, Lotz J, Seidler T, Toischer K, Zeisberg EM, Puls M, Jacobshagen C, Uecker M, Hasenfuß G, Schuster A. Real-time cardiovascular magnetic resonance T1 and extracellular volume fraction mapping for tissue characterisation in aortic stenosis. *J Cardiovasc Magn Reson*. 2020; **22**: 46.
38. Lange T, Backhaus SJ, Beuthner BE, Topci R, Rigorth KR, Kowallick JT, Evertz R, Schnelle M, Ravassa S, Díez J, Toischer K, Seidler T, Puls M, Hasenfuß G, Schuster A. Functional and structural reverse myocardial remodeling following transcatheter aortic valve replacement: a prospective cardiovascular magnetic resonance study. *J Cardiovasc Magn Reson*. 2022; **24**: 45.